Arabian Journal of Chemistry (2023) **16**, 104888

King Saud University

Arabian Journal of Chemistry

www.ksu.edu.sa
www.sciencedirect.com

ORIGINAL ARTICLE

A functional polymorphism at the miR-25-3p binding site in the 3′-untranslated region of the S1PR1 gene decreases the risk of osteoporosis in Chinese postmenopausal women

Haoyu Yang [a], Chenwei Xiong [b,c], Zhentang Yu [b,c], Zhicheng Yang [b,c], Yi Zhang [b,c], Junjie Zhang [b,c], Yong Huang [b,c], Nanwei Xu [b,c], Xindie Zhou [b,c,d,*], Mengqing Jiang [e], Zhonghua Xu [f]

[a] *Department of Orthopedics, Wuxi 9th People's Hospital affiliated to Soochow University, Wuxi 214000, China*
[b] *Department of Orthopedics, The Affiliated Changzhou Second People's Hospital of Nanjing Medical University, Changzhou 213000, China*
[c] *Changzhou Medical Center, Nanjing Medical University, Changzhou 213000, China*
[d] *Department of Orthopedics, Gonghe County Hospital of Traditional Chinese Medicine, Hainan Tibetan Autonomous Prefecture, 811800, Qinghai Province, China*
[e] *Department of pharmacy, the Second Affiliated Hospital of Jiaxing University, Jiaxing 314000, China*
[f] *Department of Orthopedics, Jintan Hospital Affiliated to Jiangsu University, Changzhou 213000, China*

Received 24 March 2022; accepted 4 April 2023
Available online 13 April 2023

KEYWORDS

MiR-25-3p;
S1PR1;
Osteoporosis;
Osteoclast;
rs41274221;
Polymorphism

Abstract The low bone mineral density due to abnormally activated osteoclasts can induce bone disorders such as osteopenia and osteoporosis. MiR-25-3p modulates sphingosine-1-phosphate receptor 1 (S1PR1) expression to enhance osteoclast motivation. The association between miR-25 rs41274221 polymorphism and osteoporosis susceptibility is unknown. Herein, 300 patients with osteoporosis and 320 healthy controls were genotyped using polymerase chain reaction and Sanger sequencing to explore the role of miR-25 rs41274221 polymorphism in osteoporosis. The odds ratios (ORs) and 95% confidence intervals (CIs) were determined using logistic regression analysis. Additionally, this study also investigated the effect of miR-25 rs41274221 polymorphism on the expression of miR-25 and its target gene S1PR1 through luciferase reporter gene, qRT-PCR, and

* Corresponding author at: Department of Orthopedics, The Affiliated Changzhou Second People's Hospital of Nanjing Medical University, Changzhou 213000, China.
E-mail address: xindiezhou@163.com (X. Zhou).
Peer review under responsibility of King Saud University.

Production and hosting by Elsevier

https://doi.org/10.1016/j.arabjc.2023.104888

Western blot. The rs41274221 in miR-25 was found to be positively associated with osteoporosis and can be viewed as a protective factor. Furthermore, miR-25 rs41274221 polymorphism decreased the risk of osteoporosis among smokers. The TargetScan database predictions and dual-luciferase activity demonstrated that S1PR1 may be the target gene of miR-25. MiR-25 down-regulated the S1PR1 mRNA and protein expressions. Patients with the AA genotype of rs41274221 polymorphism showed higher S1PR1 expression compared with the GG genotype. In conclusion, miR-25 rs41274221 polymorphism decreases the risk of osteoporosis through modifying the binding with S1PR1 and may serve as a novel biomarker for early diagnosis of osteoporosis.

1. Introduction

Osteoporosis, a frequently-occurring systemic skeletal disease, can induce bone fragility and increase the risk of fracture (Aziziyeh et al., 2019); which are associated with increased mortality and lower quality of life (Rizzoli, 2018). The prevalence of osteoporosis increases with age and is higher among women than men (Hintze and Graf, 2016). Many risk factors contribute to osteoporosis such as ethnicity, thin body, hormonal factors, smoking, less exercise, and calcium and vitamin D deficiency (Lane, 2006). Additionally, genetic background is critically involved in its occurrence (Xu et al., 2020 Oct).

MicroRNAs (miRNAs) are short non-coding RNAs that modulate gene expression by directly connecting to the 3′ untranslated region (UTR) of the corresponding messenger RNA (mRNA) (Mohr and Mott, 2015). MiRNAs participate in bone homeostasis (Tang et al., 2014), which relies on bone generation by osteoblasts and bone resorption by osteoclasts (Chen et al., 2018). Abnormal motivation of osteoclasts can decrease bone mineral density (BMD), leading to osteoporosis, osteopenia, and other bone disorders (Tang et al., 2014). For instance, MiR-874-3p promoted the osteogenic differentiation of human bone marrow mesenchymal stem cells by downregulating leptin expression (Mei et al., 2021). The role of miRNA-133a in osteoporosis modulation after menopause is to intensify osteoclast division (Li et al., 2018). miRNA-19a-3p targets HDAC4 to enhance osteogenic division of human mesenchymal stem cells and thereby relieves osteoporosis advancement (Chen et al., 2019). In addition, microRNA-7 restriction activates epidermal growth factor receptor signaling to protects human osteoblasts from dexamethasone (Fan et al., 2019). Regardless of the above achievements, the mechanisms of miRNA-mediated osteoporosis associated with osteoblasts and osteoclasts require further investigation. T The upregulation of miR-25 was observed both in the serum and bone tissue in patients with osteoporotic fractures (Seeliger et al., 2014). miR-25-3p is down-regulated in mature osteoclasts (Li et al., 2022 Jul 28). Nevertheless, little is known about the role of miR-25 in osteoclasts and osteoporosis progression.

Sphingosine-1-phosphate (S1P), a bioactive lysophospholipid concentrated in the blood, modulates the motion of osteoclast precursors between bone marrow and circulating cavities via the G-protein-coupled receptor (Ishii et al., 2011). At low S1P level, S1P receptor (S1PR)-1 mediates positive chemotaxis to S1P in the bone marrow; at high S1P level, S1PR2 regulates negative chemotaxis in the blood (Ishii et al., 2011). The S1P-S1PR1 signaling indirectly regulated bone remodeling through osteoclastogenesis and osteogenesis (Xiao et al., 2019). Moreover, the S1PRs modulator could alleviate bone loss via reducing chemotaxis of inflammatory cytokines and suppressing the receptor activator of nuclear factor NF-kB-ligand (RANKL)–induced osteoclast formation (Yu, 2021).

The TargetScan database predictions and previous sequencing results indicated that S1PR1 may be the target gene of miR-25. The miRNA-25 rs41274221 polymorphism is viewed as a pivotal genetic factor in the risks of many diseases, such as neonate sepsis (Zheng et al., 2019) and gastric cancer (Zhou et al., 2016). However, little is known about their association with osteoporosis susceptibility. In this study, we hypothesized that miR-25 rs41274221 polymorphism decreases the risk of osteoporosis through modifying the binding with S1PR1. Hence, we investigated the relationship of the miR-25 rs41274221 polymorphism with osteoporosis in postmenopausal women through in vitro and clinical study.

2. Materials and methods

2.1. Participants

A total of 300 postmenopausal women with osteoporosis and 320 age-matched volunteers were enrolled from March 2013 to June 2019 from the Jintan Hospital Affiliated with Jiangsu University. BMD was measured in the lumbar spine from vertebrae L2 to L4 and was recorded as the highest bone mass percent in the controls (T-score). Individuals with a T-score of less than −2.5 were defined as having osteoporosis. The inclusion criteria were menopause for at least one year, and taking no drugs affecting bone homeostasis.

Patients with kidney disease, cancer, pulmonary or rheumatoid disease were excluded. All participants were individuals with incidents during enrollment. This study was approved by the Institutional Ethics Committees of Jintan Hospital Affiliated with Jiangsu University. Written informed consent was acquired from the participants before participation in this study.

2.2. Genotyping

The miRNA-25 rs41274221 polymorphism was determined by the TaqMan SNP Genotyping Assay as previously described (Shen et al., 2009). Genomic DNA was extracted from peripheral venous blood (2 mL) with a QIAamp blood kit (Qiagen GmbH, Germany). Genotyping of the miR-25 polymorphisms was carried out using polymerase chain reaction (PCR). The processes were similar to those in our previous study (Zhou et al., 2016). The PCR reactions were carried out in a total volume of 5 μL containing TaqMan Universal Master Mix, SNP Genotyping Assay Mix, DNase-free water, and genomic DNA. The PCR procedure was: 50 °C, 2 min, 95 °C, 10 min; 35 cycles, 95 °C, 15 s; and 60 °C, 1 min. The 384-well ABI 7900HT Real-Time PCR System was used (ABI, CA, USA).

2.3. Osteoclast culture

The murine macrophage cell line RAW 264.7 cells were obtained from the Chinese Academy of Sciences Cell Bank

of Type Culture Collection (CBTCCCAS, Shanghai, China). The RAW 264.7 was grown in Dulbecco's Modified Eagle's Medium (DMEM, Hyclone, Logan, Utah, USA) containing 10% fetal bovine serum (Gibco, USA) in humidified 5% CO_2 at 37 °C. Cells activated with 50 ng/mL RANKL (MCE, USA) for 120 h were an extremely efficient cell model of osteoclasts (Sartori et al., 2017).

2.4. Tartrate-resistant acid phosphatase staining assay

Tartrate-resistant acid phosphatase (TRAP) staining assay was conducted as previously described (Li et al., 2022 Jul 28). Induced osteoclasts were fixed with 4% paraformaldehyde (PFA) for 20 min at room temperature and then stained with TRAP fluid (Sigma-Aldrich, Germany) for 1 h. After removal of the TRAP fluid, the plate was washed three times with phosphate-buffered saline (PBS). TRAP-positive multinuclear cells were observed using an inverted microscope.

2.5. Cell transfection

Cell transfection was conducted following the previous method (Wang et al., 2021). The miR-25-3p mimic, miR-25-3p inhibitor or negative control (NC) mimic, and NC inhibitor used in this study were designed and synthesized by GenePharma, China. Before transfection, a mixture of miR-25-3P mimics, inhibitor, and NC was centrifuged at 2000 rpm for 10 min, then 250 μL RNase-free H_2O was added to dissolve the mixture to 20 μM, and finally was stored at − 20 °C. When the cells reached 80 % of the plates, the cells were transfected with Opti-MEM (Gibco-BRL Co. LTD), NC, miR-25-3P mimics, and miR-25-3P inhibitor using Lipofectamine 3000 (Invitrogen, Carlsbad, USA) according to the manufacturer's instructions. Cells were collected after 48 h for RNA extraction.

2.6. Cell Counting Kit-8 assay

Cell proliferation was detected using Cell Counting Kit-8 (CCK-8) as previously described (Li et al., 2022 Jul 28). Cells (n = 1000) were seeded into 96-well plates and cultured for the indicated times. CCK-8 (Dojindo Molecular Technology, Japan) was added, and cells were incubated for an additional 2 h at 37℃, followed by detection at 450 nm (650nmreference) on an ELx800 absorbance microplate reader (Biotek Instruments, Winooski, VT, USA).

2.7. Dual-luciferase activity

A luciferase reporter assay was performed according to the previous study (Li et al., 2022 Jan). The HEK293T (human embryonic kidney-CRL3216) cells were obtained commercially from ATCC. The pGL3 vector (Promega Corporation, Madison, USA) and the synthetic S1PR1 with wild-type (WT) or mutated (Mut) region were adopted to construct the reporter plasmids of S1PR1-WT/Mut. Subsequently, the reporter plasmids and miR-25 mimic were co-transfected into HEK293T through Lipofectamine 2000. MiR-NC was used as the negative control. Next, the Dual-Luciferase Reporter Gene Assay System was used to estimate the Renilla and Firefly luciferase activities after 48 h.

2.8. Quantitative reverse-transcription polymerase chain reaction

The quantitative real-time PCR (qRT-PCR) was performed according to the previous study (Zhou et al., 2020 Oct 25). Total RNA was isolated from harvested cells using a Trizol reagent (Invitrogen, USA) as instructed in the manual. The reaction system was configured according to the instruction of the reverse transcription kit. The reaction conditions were: 42 °C 15 min, 95 °C 3 min. The cDNA was synthesized by reverse transcription and amplified by qRT-PCR. The expressions of corresponding mRNAs in the reaction system were detected by fluorescence quantitative PCR according to the instruction of SYBR Green Kit. Glyceraldehyde-3-phosphate dehydrogenase (GAPDH) was used as an internal control. MiR-specific qRT-PCR was carried out, and miRNAs were quantified with U6 small nuclear RNA (sncU6) as a control (Clontech, USA). The forward and reverse primer sequences used were: 5′-GCCTCTCCAGCCAAGGAAAA-3′, 5′-GGAGCCTGGGGTGGTATTTC-3′ (S1PR1); 5′-GGCTGTATTCCCCTCCATCG-3′, 5′-CCAGTTGGTAACAATGCCATGT-3′ (GAPDH); 5′-ACTCCACATTGCACTTGTCTCG-3′, 5′-GTGCAGGGTCCGAGGT-3′ (miR-25); 5′-CTCGCTTCGGCAGCACA-3′, 5′-AACGCTTCACGAATTTGCGT-3′ (U6).

2.9. Western blot

Western blotting was conducted as previously described (Zhou et al., 2019 Jun). Total proteins were isolated from osteoclast cell lysates and quantified in each specimen using a BCA kit (Beyotime Biotechnology, China). The proteins were separated by sodium dodecyl sulfate–polyacrylamide gel electrophoresis and then removed to PVDF membranes. After blocking with 5% skim milk for 2 h, the membranes were cultured first with the primary antibody anti-S1PR1 and then with horseradish peroxidase-conjugated secondary antibody (cat. no. ab205718; 1:2000). The protein bands were observed by Image Quant TL and analyzed with ImageJ.

2.10. Immunofluorescence analysis

The procedure of immunofluorescence analysis was almost the same as in a previous study (Liu et al., 2019). After reaching a confluence of more than 80%, the original medium was discarded, and the cells were washed once with PBS. After the addition of a basal medium, cells were starved for 20 min, and a transfection mixture was added for 6 h of incubation. Then, a RANKL medium was used for 120 h. After the replacement of the complete medium, the cells were fixed with formaldehyde. The fixed cells were permeated with 0.1% Triton X-100 for 10 min and washed with PBS. Then the cells in PBS containing 1% BSA were treated overnight with the primary antibody against S1PR1 at 4 °C. Next, the secondary antibody conjugated with Alexa Fluor 594 (Cell Signaling Technology) was added at ambient temperature. After the nuclei were dyed with DAPI (Thermo Fisher Scientific) for 5 min, the coverslip was fastened on the glass slide and the cells were visualized under a Leica fluorescence microscope.

2.11. Statistical analysis

All statistical analyses were completed on SAS V9 (SAS Institute, USA). Conformation of allele frequencies to the Hardy–Weinberg equilibrium (HWE) was assessed by Chi-square test. Demographic differences between groups were compared by Student's *t* test (continuous data) or Chi-square test (categorical data). Clinical differences as per genotypes were examined by analysis of variance. Odds ratio (OR) and 95% confidence interval (CI) were computed to assess the relationship between genetic variants and osteoporosis risk through logistic regression analysis in the 5 models. The cut-off point for statistical significance was alpha < 0.05. All statistical results of functional experiments are from more than three repeated experiments.

3. Results

In the current study, we hypothesized that miR-25 rs41274221 polymorphism decreases the risk of osteoporosis through modifying the binding with S1PR1. Hence, we investigated the relationship of the miR-25 rs41274221 polymorphism with osteoporosis through in vitro and clinical study. The results showed that the rs41274221 in miR-25 can be viewed as a protective factor that decreased the risk of osteoporosis in postmenopausal women, and S1PR1 may be the target gene involved in the regulation of osteoporosis. Furthermore, subgroup analyses demonstrated that the miR-25rs41274221 polymorphism was associated with a reduced risk of osteoporosis in smokers.

Table 1 Patient demographics and risk factors in osteoporosis.

Characteristics	Case (N = 300)	Control (N = 320)	*P*
Age, years	62.78 ± 8.53	62.57 ± 8.25	0.761
BMI, kg/m^2	24.40 ± 1.45	24.27 ± 1.50	0.253
Smoking			
No/Yes	241/59	266/54	0.368
Serum calcium	9.31 ± 0.65	9.56 ± 0.57	< 0.001
LBMD, g/cm^2	0.73 ± 0.07	1.01 ± 0.06	< 0.001
T-score	−3.19 ± 0.39	0.12 ± 0.10	< 0.001

BMI, body mass index; LBMD, lumbar spine BMD.

3.1. Baseline characteristics

Characteristics of the participants are shown in Table 1. No significant discrepancy between groups was observed with respect to age (62.78 vs. 62.57 years), BMI (24.40 vs. 24.27 kg/m^2), or the proportion of smoking or drinking. Positive results were observed in BMD L2-L4, T-scores, and serum calcium (all $P < 0.001$).

3.2. MiR-25 SNP and osteoporosis susceptibility

The details of rs41274221 polymorphism in miR-25 are summarized in Table 2. The frequencies of the GG, AG, and AA genotypes of miR-25 rs41274221 among the controls are 46.9%, 42.5%, and 10.6% respectively, which conform to the HWE. Our results indicate that genotype AA, rather than genotype GA, has lower susceptibility to osteoporosis compared with genotype GG (AA vs. GG: OR, 0.55; 95% CI: 0.30–0.99; $P = 0.046$). Allele A versus allele G is related to a significantly lower risk of osteoporosis (OR: 0.76; 95% CI: 0.60–0.98; $P = 0.032$). No significant connection with osteoporosis risk is noted in other models for rs41274221 polymor-

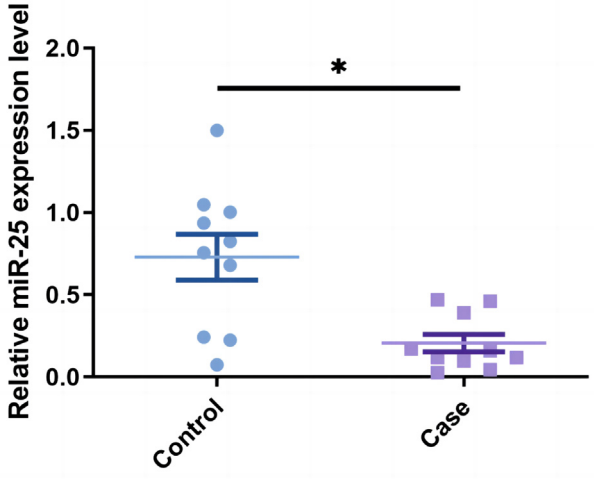

Fig. 1 Relative miR-25 mRNA expression level in osteoporosis patients and healthy samples, as analyzed by qRT-PCR, * $P < 0.05$.

Table 2 Genotype frequencies of miR-25 rs41274221 polymorphism in cases and controls.

Models	Genotype	Case (n, %)	Control (n, %)	OR (95% CI)	*P*-value	*OR (95% CI)	**P*-value
Wild	GG	162 (54.0%)	150 (46.9%)	1.0			
Heterozygote	GA	118 (39.3%)	136 (42.5%)	0.80(0.58,1.12)	0.196	0.80(0.57,1.12)	0.190
Homozygote	AA	20 (6.7%)	34 (10.6%)	**0.55(0.30,0.99)**	**0.046**	**0.55(0.30,0.99)**	**0.047**
Dominant	GG	162 (54.0%)	150 (46.9%)	1.0			
	GA + AA	138 (46.0%)	170 (53.1%)	0.75(0.55,1.03)	0.076	0.75(0.55,1.03)	0.075
Recessive	GG + GA	280 (93.3%)	286 (89.4%)	1.0			
	AA	20 (6.7%)	34 (10.6%)	0.60(0.34,1.07)	0.083	0.60(0.34,1.08)	0.087
Allele	G	442 (73.7%)	436 (68.1%)	1.0			
	A	158 (26.3%)	204 (31.9%)	**0.76(0.60,0.98)**	**0.032**		

Bold values are statistically significant (P < 0.05).
*Adjust for age and body mass index.

phism. In addition, to assess the differences in miR-25 expression in healthy subjects and osteoporosis patients, qRT-PCR analysis of blood samples was performed with 10 patients and 10 controls. The results showed that miR-25 expression was significantly downregulated in osteoporosis patients as compared with healthy subjects (Fig. 1).

Subgroup analyses were conducted according to age, BMI, and smoking (Table 3). Genotype AA in osteoporosis patients was significantly more frequent among smokers than in the controls. In other words, miR-25 rs41274221 polymorphism is linked with a lower risk of osteoporosis among smokers. Finally, clinical features in different genotypes are presented in Table 4. No evidence of association was observed between rs41274221 polymorphism and age, BMI, serum calcium, LBMD, or T-score.

3.3. MiR-25 negatively regulated S1PR1 expression in osteoclasts

To clarify the biological effects of MiR-25-3p in the osteoclast differentiation of RAW264.7, we performed a CCK-8 assay, and TRAP staining to determine the proliferation and differentiation of osteoclasts. The results showed that the anti–miR-25-3p increased osteoclast proliferation as compared to the control group, while the miR-25-3p significantly inhibited the osteoclast proliferation (Fig. 2a). Then, we fixed the osteoclasts and performed TRAP staining. The results showed a significant increase in the number of TRAP-positive osteoclasts in the anti–mir-25-3p–treated group and a significant decrease in the miR-25-3p–treated group compared to control cells (Fig. 2b). The above results confirmed that miR-25-3p significantly inhibited osteoclast proliferation and differentiation in vitro. Besides, we observed miR-25-3p downregulation in mature osteoclasts (Li et al., 2022 Jul 28). Then we examined the effect of miR-25 on S1PR1 expression in osteoclasts. Cells with remarkable upregulation or downregulation of miR-25 relative to the negative control were acquired by transfection with miR-25 mimics (Fig. 3a). Knockdown of miR-25 improved S1PR1 mRNA and protein expressions in osteoclasts (Fig. 3b, 3c, and 3d). When the miR-25 level is elevated, the negative regulatory relationship remains in effect.

The intensity of S1PR1 in RANKL-activated RAW 264.7 at miR-25 inhibitor/mimics was measured by immunofluorescence assay. The fluorescence intensity of S1PR1 was significantly lower in the miR-25 mimics group and was higher in the miR-25 inhibitor group than in the control group (Fig. 4a and 4b). These results indicate the S1PR1 expression and miR-25 expression are negatively related. The dual-luciferase assay was performed to evaluate whether S1PR1 is a target gene of miR-25. Our results indicated that the relative luciferase activity differed significantly between the S1PR1-Mut and the S1PR1-WT group which were both co-treated with miR-25 mimic (Fig. 5, $P < 0.05$). This result confirmed that there was a direct interaction between miR-25 and S1PR1.

Hence, we believe the SNP in the mature zone of miR-25 may abnormally attenuate the action induced by miR-25 in modulating S1PR1. We also detected S1PR1 expression in patients carrying discrepant genotypes of miR-25. The patients with genotype AA show an increase in S1PR1 expression (Fig. 6).

Table 3 Stratified analyses between miR-25 rs41274221 polymorphism and the risk of osteoporosis.

Variable	case/control			Heterozygous	Homozygous	Recessive	Dominant
	GG	GA	AA	GA vs. GG OR (95% CI), *P* value	AA vs. GG OR (95% CI), *P* value	AA vs. GA + GG OR (95% CI), *P* value	AA + GA vs. GG OR (95% CI), *P* value
Age (years)							
< 60	61/58	45/58	9/15	0.74(0.43,1.25); 0.261	0.57(0.23,1.41); 0.222	0.66(0.28,1.56); 0.342	0.70(0.43,1.16); 0.170
≥ 60	101/92	73/78	11/19	0.85(0.56,1.31); 0.463	0.53(024,1.17); 0.114	0.57(0.26,1.22); 0.148	0.79(0.53,1.18); 0.253
BMI (kg/m2)							
< 25	109/109	77/89	14/23	0.87(0.58,1.30); 0.483	0.61(0.30,1.25); 0.174	0.65(0.32,1.30); 0.220	0.81(0.55,1.19); 0.289
≥ 25	53/41	41/47	6/11	0.68(0.38,1.21); 0.187	0.42(0.14,1.24); 0.116	0.51(0.18,1.44); 0.204	0.63(0.36,1.10); 0.102
Smoking							
No	125/128	97/114	19/24	0.87(0.60,1.26); 0.461	0.81(0.42,1.55); 0.527	0.86(0.46,1.62); 0.646	0.86(0.61,1.22); 0.400
Yes	37/22	21/22	1/10	0.57(0.26,1.26); 0.164	**0.06(0.01,0.50); 0.009**	**0.08(0.01,0.62); 0.016**	**0.41(0.19,0.87); 0.021**

Bold values are statistically significant ($P < 0.05$).

Table 4 The clinical and biochemical characteristics of miR-25 rs41274221 polymorphism among two groups.

Variables	Patients(N = 300)				Controls(N = 320)			
	GG (N = 162)	GA (N = 118)	AA (N = 20)	*P*	GG (N = 188)	GA (N = 167)	AA (N = 36)	*P*
Age, years	63.33 ± 8.75	62.42 ± 8.47	60.40 ± 6.75	0.294	62.92 ± 8.33	62.40 ± 8.14	61.71 ± 8.47	0.707
BMI, kg/m^2	24.46 ± 1.39	24.37 ± 1.50	24.14 ± 1.66	0.618	24.11 ± 1.57	24.41 ± 1.46	24.37 ± 1.34	0.213
Serum calcium	9.27 ± 0.65	9.37 ± 0.69	9.26 ± 0.49	0.405	9.58 ± 0.58	9.54 ± 0.56	9.56 ± 0.56	0.841
LBMD, g/cm^2	0.72 ± 0.06	0.73 ± 0.07	0.75 ± 0.08	0.140	1.01 ± 0.06	1.01 ± 0.05	1.03 ± 0.06	0.212
T-score	−3.16 ± 0.40	−3.21 ± 0.37	−3.27 ± 0.38	0.340	0.12 ± 0.09	0.11 ± 0.10	0.13 ± 0.11	0.611

Bold values are statistically significant ($P < 0.05$).

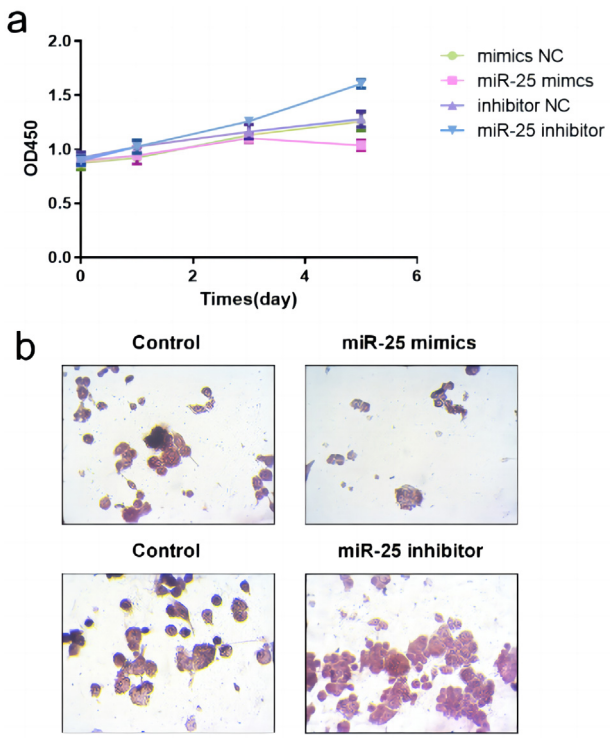

Fig. 2 (a) RAW 264.7 cells were cultured in a-MEM containing RANKL (50 ng/mL) for 120 h. The CCK-8 assay was used to detect proliferation. (b) Representative pictures of TRAP-positive multinucleated cells are shown.

4. Discussion

Although miRNAs are known to modulate the differentiation and roles of skeletal cells, the knowledge of miRNA SNPs in osteoporosis is still largely lacking. In miRNA genes and miRNA-binding places, SNPs can alter miRNA level and mRNA targeting (Dole and Delany, 2016). This study established that miR-25 is significantly associated with osteoporosis in postmenopausal women and may be a protective factor. Like other studies on gastric cancer, we also demonstrate that miR-25 may be weakened by miR-25 rs41274221 owing to the blockade at the 3′-UTR of S1PR1.

S1P signaling, via its cell surface receptor S1PR1, can activate the growth, spread, living, angiogenesis, and migration of cancer cells and accelerate tumorigenesis (Rostami et al., 2019). S1P signaling also plays an important role in immune cells and inflammation (Aoki et al., 2016), multiple sclerosis (Cohan et al., 2020), and viral infection (Li et al., 2016). Therefore, we throw light on the effect of S1P-S1PRs signaling on the mechanism of osteoporosis. S1P, which is abundant in blood, modulates the movement of osteoclast precursors between the circulation and bone marrow cavities via G-protein-bound receptors (S1PR1 and S1PR2) (Ishii and Kikuta, 2013). S1PR2 inhibition can limit osteoclast precursor localization and reduce the number of mature osteoclasts bound to bone surface (Ishii et al., 2010). Nevertheless, the role of S1PR1 in osteoporosis is yet unclear. In this study, we quantified miR-25 expression from the plasma of osteoporosis patients and healthy subjects, and found that miR-25 expres-

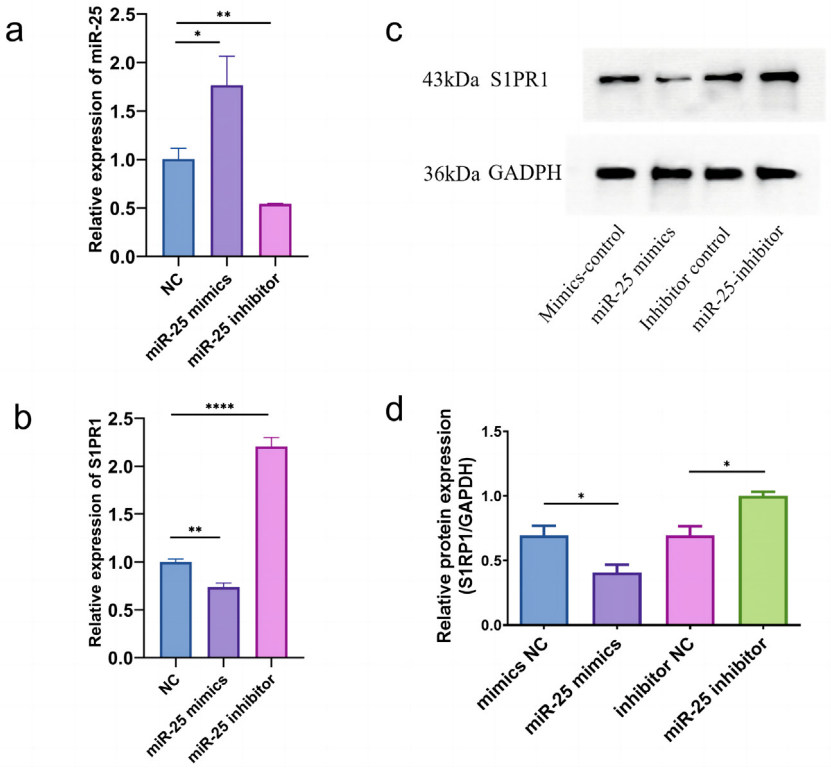

Fig. 3 Levels of miR-25 and S1PR1 in HEK293T cell transfected with different miR-25 mimics/inhibitors. Relative levels of (a) miR-25-3p and (b) S1PR1 after transfection of miR-25-3p or anti-miR-25-3p measured by qRT-PCR. (c) The protein band of western blotting for S1PR1. (d) The analysis for gray value by Image J. Data represent mean ± SD (n = 3), * $P < 0.05$, ** $P < 0.01$ and **** $P < 0.0001$ vs. the control group.

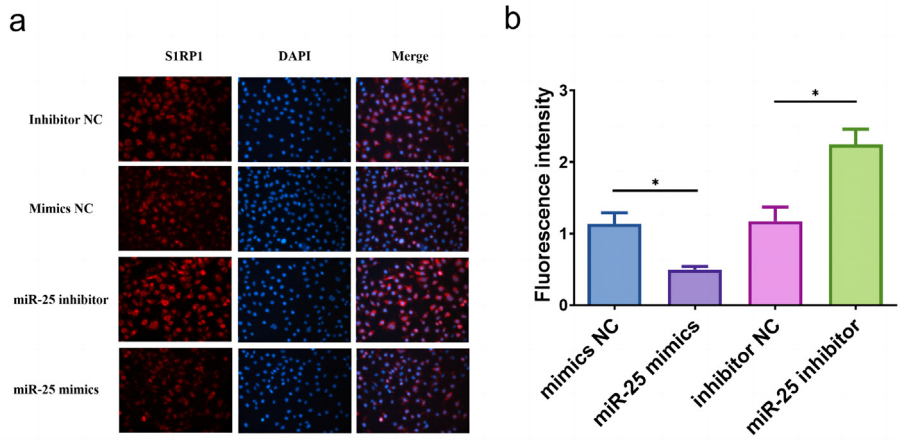

Fig. 4 (a) Representative immunofluorescence photomicrograph of S1PR1 (red)-labeled osteoclasts. Nuclei were stained with DAPI (blue). (b) Fluorescence quantitative histogram of photomicrograph, * $P < 0.05$.

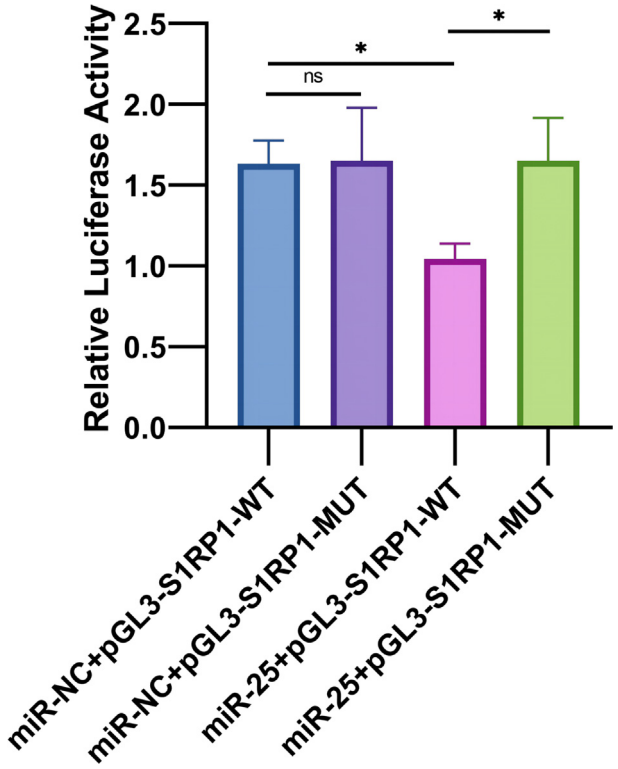

Fig. 5 The dual-luciferase assay demonstrated the existence of direct interaction between miR-25 and S1PR1, * $P < 0.05$.

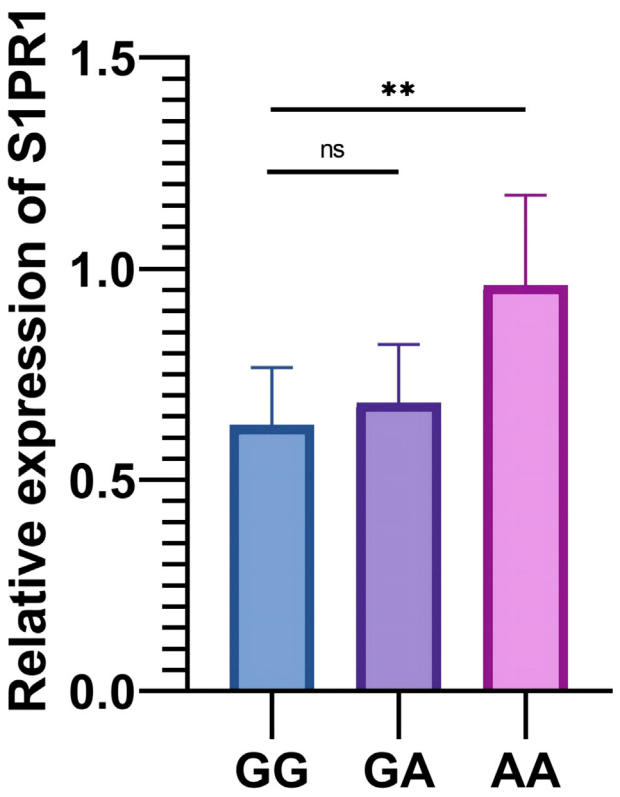

Fig. 6 S1PR1 expression in different genotypes of rs41274221 polymorphism, ** $P < 0.01$.

sion was significantly lower in OA patients than in healthy subjects. The CCK-8 assay and TRAP staining confirmed that miR-25-3p significantly inhibited osteoclast proliferation and differentiation in vitro. In osteoclasts, the mRNA and protein expression of S1PR1 is negatively regulated by miR-25. A dual-luciferase reporter assay confirmed that S1PR1 is a target gene of miR-25. Additionally, the S1PR1 expression in individuals with the GG genotype is significantly lower than that of the AA genotype. Therefore, we speculate that the SNP on mir-25 affects the binding to the 3′-UTR of S1PR1, thus influencing the expression of S1PR1.

SNPs in miRNA-binding sites lower or raise the target mRNA translation by impacting the linking of miRNAs with the target genes, and thus are associated with susceptibility to diseases (Liu et al., 2018; Shasttiri et al., 2019). The SNP rs41274221 in miR-25 is reportedly involved in the incidence of gastric cancer by playing a tumor protective role related to tumor growth and metastasis (Zhou et al., 2016). Conse-

quently, this polymorphism is also related to the risk of sepsis in newborns (Zheng et al., 2019). Therefore, our group conducted this study to evaluate whether this association was significant in osteoporosis. Polymorphism in miR-25 rs41274221 is positively correlated with osteoporosis susceptibility, which is similar to previous studies (Zheng et al., 2019; Zhou et al., 2016). Subgroup analyses revealed that miR-25 rs41274221 polymorphism is connected to the decreased risk of osteoporosis among smokers.

There are several potential limitations in our study. First, the moderate sample size may reduce the statistical power. Second, we failed to conduct more subgroup analyses due to limited clinical information, such as drinking and physical activity. Third, a small number of patients, especially only participants in China were recruited, so it is yet to be known how these findings would apply to other ethnicities.

5. Conclusion

In conclusion, the SNP rs41274221 in miR-25, by interfering with the modulation target of S1PR1, may be a protective factor in the pathogenesis of osteoporosis in postmenopausal women. However, due to the limitation of region, as well as the number of participants, we believe that further research with larger populations is called for to verify the connection and assess the roles of this polymorphism.

Funding

This study was supported by Changzhou Sci&Tech Program (Grant No. CJ20220120, CJ20210104, CJ20210003 and CJ20210005), Funding from Young Talent Development Plan of Changzhou Health Commission (CZQM2020059), Top Talent of Changzhou "The 14th Five-Year Plan" High-Level Health Talents Training Project (2022CZBJ059 and 2022CZBJ061) and Qinghai Province Health System Guidance Plan Project (2022-wjzdx-106).

CRediT authorship contribution statement

Haoyu Yang: Data curation, Writing – original draft. **Chenwei Xiong:** Visualization, Investigation, Writing – review & editing. **Zhentang Yu:** Conceptualization, Methodology, Software. **Zhicheng Yang:** Data curation, Writing – original draft. **Yi Zhang:** Visualization, Investigation. **Junjie Zhang:** Supervision, Software, Validation. **Yong Huang:** Supervision, Software, Validation. **Nanwei Xu:** Supervision, Software, Validation. **Xindie Zhou:** Conceptualization, Methodology, Software, Writing – review & editing. **Mengqing Jiang:** Conceptualization, Methodology, Software. **Zhonghua Xu:** .

Declaration of Competing Interest

The authors declare that they have no known competing financial interests or personal relationships that could have appeared to influence the work reported in this paper.

References

Aoki, M., Aoki, H., Ramanathan, R., Hait, N.C., Takabe, K., 2016. Sphingosine-1-phosphate signaling in immune cells and inflammation: roles and therapeutic potential. Mediators Inflamm. 2016, 8606878.

Aziziyeh, R., Amin, M., Habib, M., Garcia Perlaza, J., Szafranski, K., McTavish, R.K., et al, 2019. The burden of osteoporosis in four Latin American countries: Brazil, Mexico, Colombia, and Argentina. J. Med. Econ. 22 (7), 638–644.

Chen, R., Qiu, H., Tong, Y., Liao, F., Hu, X., Qiu, Y., et al, 2019. MiRNA-19a-3p alleviates the progression of osteoporosis by targeting HDAC4 to promote the osteogenic differentiation of hMSCs. Biochem. Biophys. Res. Commun. 516 (3), 666–672.

Chen, X., Wang, Z., Duan, N., Zhu, G., Schwarz, E.M., Xie, C., 2018. Osteoblast-osteoclast interactions. Connect. Tissue Res. 59 (2), 99–107.

Cohan, S., Lucassen, E., Smoot, K., Brink, J., Chen, C., 2020. Sphingosine-1-phosphate: its pharmacological regulation and the treatment of multiple sclerosis: a review article. Biomedicines 8 (7).

Dole, N.S., Delany, A.M., 2016. MicroRNA variants as genetic determinants of bone mass. Bone 84, 57–68.

Fan, J.B., Liu, W., Zhu, X.H., Cui, S.Y., Cui, Z.M., Zhao, J.N., 2019. microRNA-7 inhibition protects human osteoblasts from dexamethasone via activation of epidermal growth factor receptor signaling. Mol. Cell. Biochem. 460 (1–2), 113–121.

Hintze, G., Graf, D., 2016. Osteoporosis. Med. Monatsschr. Pharm. 39 (6), 228–234.

Ishii, M., Kikuta, J., 2013. Sphingosine-1-phosphate signaling controlling osteoclasts and bone homeostasis. Biochim. Biophys. Acta 1831 (1), 223–227.

Ishii, M., Kikuta, J., Shimazu, Y., Meier-Schellersheim, M., Germain, R.N., 2010. Chemorepulsion by blood S1P regulates osteoclast precursor mobilization and bone remodeling in vivo. J. Exp. Med. 207 (13), 2793–2798.

Ishii, T., Shimazu, Y., Nishiyama, I., Kikuta, J., Ishii, M., 2011. The role of sphingosine 1-phosphate in migration of osteoclast precursors; an application of intravital two-photon microscopy. Mol. Cells 31 (5), 399–403.

Lane, N.E., 2006. Epidemiology, etiology, and diagnosis of osteoporosis. Am. J. Obstet. Gynecol. 194 (2 Suppl), S3–S.

Li Y, Xie P, Sun M, Xiang B, Kang Y, Gao P, et al. S1PR1 expression correlates with inflammatory responses to Newcastle disease virus infection. Infection, genetics and evolution : journal of molecular epidemiology and evolutionary genetics in infectious diseases. 2016;37:37-42

Li, J., Jiang, M., Xiong, C., Pan, J., Jia, S., Zhang, Y., et al, 2022 Jan. KLF4, negatively regulated by miR-7, suppresses osteoarthritis development via activating TGF-β1 signaling. Int. Immunopharmacol. 102, 108416.

Li, J., Jiang, M., Yu, Z., Xiong, C., Pan, J., Cai, Z., et al, 2022 Jul 28. Artemisinin relieves osteoarthritis by activating mitochondrial autophagy through reducing TNFSF11 expression and inhibiting PI3K/AKT/mTOR signaling in cartilage. Cell. Mol. Biol. Lett. 27 (1), 62.

Li, Z., Zhang, W., Huang, Y., 2018. MiRNA-133a is involved in the regulation of postmenopausal osteoporosis through promoting osteoclast differentiation. Acta Biochim. Biophy. Sin. 50 (3), 273–280.

Liu, B., Li, X., Li, C., Xu, R., Sun, X., 2019. miR-25 mediates metastasis and epithelial-mesenchymal-transition in human esophageal squamous cell carcinoma via regulation of E-cadherin signaling. Bioengineered 10 (1), 679–688.

Liu, X., Wang, L., Chi, H., Wang, J., Zheng, Q., Li, J., et al, 2018. The SNP Rs915014 in MTHFR regulated by MiRNA associates with atherosclerosis. Cell. Physiol. Biochem. 45 (3), 1149–1155.

Mei, L., Li, M., Zhang, T., 2021. MicroRNA miR-874-3p inhibits osteoporosis by targeting leptin (LEP). Bioengineered 12 (2), 11756–11767.

Mohr, A.M., Mott, J.L., 2015. Overview of microRNA biology. Semin. Liver Dis. 35 (1), 3–11.

Rizzoli, R., 2018. Postmenopausal osteoporosis: assessment and management. Best Pract. Res. Clin. Endocrinol. Metab. 32 (5), 739–757.

Rostami, N., Nikkhoo, A., Ajjoolabady, A., Azizi, G., Hojjat-Farsangi, M., Ghalamfarsa, G., et al, 2019. S1PR1 as a novel promising therapeutic target in cancer therapy. Mol. Diagn. Ther. 23 (4), 467–487.

Sartori, M., Vincenzi, F., Ravani, A., Cepollaro, S., Martini, L., Varani, K., et al, 2017. RAW 264.7 co-cultured with ultra-high molecular weight polyethylene particles spontaneously differentiate into osteoclasts: an in vitro model of periprosthetic osteolysis. J. Biomed. Mater. Res. A 105 (2), 510–520.

Seeliger, C., Karpinski, K., Haug, A.T., Vester, H., Schmitt, A., Bauer, J.S., et al, 2014. Five freely circulating miRNAs and bone tissue miRNAs are associated with osteoporotic fractures. J. Bone Miner. Res. 29 (8), 1718–1728.

Shasttiri, A., Rostamian Delavar, M., Baghi, M., Dehghani Ashkezari, M., Ghaedi, K., 2019. SNP rs10800708 within the KIF14 miRNA binding site is linked with breast cancer. Br. J. Biomed. Sci. 76 (1), 46–48.

Shen, G.Q., Abdullah, K.G., Wang, Q.K., 2009. The TaqMan method for SNP genotyping. Methods Mol. Biol. (Clifton, NJ) 578, 293–306.

Tang, P., Xiong, Q., Ge, W., Zhang, L., 2014. The role of microRNAs in osteoclasts and osteoporosis. RNA Biol. 11 (11), 1355–1363.

Wang, X., Sun, H., Zhu, S., 2021. Long non-coding RNA PTAR inhibits apoptosis but promotes proliferation, invasion and migration of cervical cancer cells by binding miR-101. Bioengineered 12 (1), 4536–4545.

Xiao, L., Zhou, Y., Friis, T., Beagley, K., Xiao, Y., 2019. S1P–S1PR1 signaling: the "Sphinx" in osteoimmunology. Front. Immunol. 10, 1409.

Xu, Z., He, J., Zhou, X., Zhang, Y., Huang, Y., Xu, N., et al, 2020 Oct. Down-regulation of LECT2 promotes osteogenic differentiation of MSCs via activating Wnt/β-catenin pathway. Biomed. Pharmacother. 130, 110593.

Yu, H., 2021. Targeting S1PRs as a therapeutic strategy for inflammatory bone loss diseases-beyond regulating S1P signaling. Int. J. Mol. Sci. 22 (9).

Zheng, G., Xiang, W., Pan, M., Huang, Y., Li, Z., 2019. Identification of the association between rs41274221 polymorphism in the seed sequence of microRNA-25 and the risk of neonate sepsis. J. Cell. Physiol.

Zhou, X., Jiang, L., Fan, G., Yang, H., Wu, L., Huang, Y., et al, 2019 Jun. Role of the ciRS-7/miR-7 axis in the regulation of proliferation, apoptosis and inflammation of chondrocytes induced by IL-1β. Int. Immunopharmacol. 71, 233–240.

Zhou, X., Li, J., Zhou, Y., Yang, Z., Yang, H., Li, D., et al, 2020 Oct 25. Down-regulated ciRS-7/up-regulated miR-7 axis aggravated cartilage degradation and autophagy defection by PI3K/AKT/mTOR activation mediated by IL-17A in osteoarthritis. Aging (Albany NY) 12 (20), 20163–20183.

Zhou, J., Zhou, J., Wang, W., Li, W., Wu, L., Li, G., et al, 2016. The polymorphism in miR-25 attenuated the oncogenic function in gastric cancer. Tumour Biol. : J. Int. Soc. Oncodevelop. Biol. Med. 37 (4), 5515–5520.